



Biomolecules and Biomedicine
ISSN: 2831-0896 (Print) | ISSN: 2831-090X (Online)

Journal Impact Factor® (2021): 3.76

CiteScore® (2021): 5.2

www.biomolbiomed.com | blog.biomolbiomed.com

SUPPLEMENTAL DATA

A novel autophagy-related subtypes to distinguish immune phenotypes and predict immunotherapy response in head and neck squamous cell carcinoma

Table S1. Basic information of datasets included in this study for identifying distinct autophagy-related patterns.

ID	Tumor type	Sample			Platform
		Total	Tumor	Non-tumor	
E-MTAB-1328	HNSCC	89	89	-	GPL570 Affymetrix Human Genome U133 Plus 2.0 Array
GSE39366	HNSCC	138	138	-	GPL9053 Agilent-UNC-custom-4X44K
GSE41613	OSCC	97	97	-	GPL570 Affymetrix Human Genome U133 Plus 2.0 Array
GSE42743	OSCC	103	109	-	GPL570 Affymetrix Human Genome U133 Plus 2.0 Array
GSE65858	HNSCC	270	270	-	GPL10558 Illumina HumanHT-12 V4.0 expression beadchip
E-TABM-302	HNSCC	81	81	-	GPL570 Affymetrix Human Genome U133 Plus 2.0 Array
GSE6791	Head/Neck and Cervical Cancers	84	42	14	GPL570 Affymetrix Human Genome U133 Plus 2.0 Array

ID	Tumor type	Sample			Platform
		Total	Tumor	Non-tumor	
GSE30784	OSCC	229	167	62	GPL570 Affymetrix Human Genome U133 Plus 2.0 Array
GSE40774	HNSCC	134	134	-	GPL13497 Agilent-026652 Whole Human Genome Microarray 4x44K v2
GSE84846	OSCC	99	99	-	GPL6480 Agilent-014850 Whole Human Genome Microarray 4x44K G4112F
E-MTAB-1328	HNSCC	89	89	-	GPL570 Affymetrix Human Genome U133 Plus 2.0 Array

Table S2. Summary of detailed clinical information of TCGA-HNSCC cohort.

TCGA-BLCA	Low (n=226)	High (n=272)	Total (n=498)	P value
Age				0.639
<= 65	144 (63.7%)	179 (65.8%)	323 (64.9%)	
> 65	82 (36.3%)	93 (34.2%)	175 (35.1%)	
Sex				0.542
Female	63 (27.9%)	69 (25.4%)	132 (26.5%)	
Male	163 (72.1%)	203 (74.6%)	366 (73.5%)	
Vital status***				<0.00001
Dead	74 (32.7%)	143 (52.6%)	217 (43.6%)	
Alive	152 (67.3%)	129 (47.4%)	281 (56.4%)	
Primary therapy outcome**				0.006219
CR	172 (76.1%)	181 (66.5%)	353 (70.9%)	

TCGA-BLCA	Low (n=226)	High (n=272)	Total (n=498)	P value
PR	2 (0.9%)	4 (1.5%)	6 (1.2%)	
SD	2 (0.9%)	3 (1.1%)	5 (1.0%)	
PD	9 (4.0%)	34 (12.5%)	43 (8.6%)	
Follow-up treatment outcome				0.182
CR	104 (46.0%)	108 (39.7%)	212 (42.6%)	
PR	2 (0.9%)	3 (1.1%)	5 (1.0%)	
SD	2 (0.9%)	5 (1.8%)	7 (1.4%)	
PD	33 (14.6%)	53 (19.5%)	86 (17.3%)	
Lymph nodes positive by HE				0.9169
>0	95 (42.0%)	135 (49.6%)	230 (46.2%)	
0	65 (28.8%)	95 (34.9%)	160 (32.1%)	
Lymphovascular invasion				1

TCGA-BLCA	Low (n=226)	High (n=272)	Total (n=498)	P value
No	92 (40.7%)	126 (46.3%)	218 (43.8%)	
Yes	51 (22.6%)	69 (25.4%)	120 (24.1%)	
Histological grade**				0.00687
G1	28 (12.4%)	32 (11.8%)	60 (12.0%)	
G2	116 (51.3%)	182 (66.9%)	298 (59.8%)	
G3	68 (30.1%)	51 (18.8%)	119 (23.9%)	
G4	2 (0.9%)	0 (0%)	2 (0.4%)	
Molecular subtype***				<0.00001
Atypical	60 (26.5%)	8 (2.9%)	68 (13.7%)	
Basal	28 (12.4%)	56 (20.6%)	84 (16.9%)	
Classical	5 (2.2%)	44 (16.2%)	49 (9.8%)	
Mesenchymal	42 (18.6%)	33 (12.1%)	75 (15.1%)	

TCGA-BLCA	Low (n=226)	High (n=272)	Total (n=498)	P value
Pathologic T stage**				0.0062
T0-T2	90 (39.8%)	87 (32.0%)	177 (35.5%)	
T3-T4	100 (44.2%)	166 (61.0%)	266 (53.4%)	
Pathologic N stage				0.6109
N0	75 (33.2%)	94 (34.6%)	169 (33.9%)	
N1-N3	98 (43.4%)	138 (50.7%)	236 (47.4%)	
Pathologic M stage				1
M0	88 (38.9%)	97 (35.7%)	185 (37.1%)	
M1	0 (0%)	1 (0.4%)	1 (0.2%)	
Pathologic TNM stage*				0.0263
I-II	51 (22.6%)	46 (16.9%)	97 (19.5%)	
III-IV	132 (58.4%)	204 (75.0%)	336 (67.5%)	

TCGA-BLCA	Low (n=226)	High (n=272)	Total (n=498)	P value
Neoplasm_cancer_status*				0.0198
Tumor-free	155 (68.6%)	156 (57.4%)	311 (62.4%)	
With tumor	62 (27.4%)	99 (36.4%)	161 (32.3%)	
Alcohol_history				1
No	71 (31.4%)	85 (31.2%)	156 (31.3%)	
Yes	151 (66.8%)	180 (66.2%)	331 (66.5%)	
HPV Status***				<0.00001
Negative	160 (70.8%)	249 (91.5%)	409 (82.1%)	
Positive	66 (29.2%)	23 (8.5%)	89 (17.9%)	
Margin status				0.865135
Close	19 (8.4%)	30 (11.0%)	49 (9.8%)	
Negative	143 (63.3%)	197 (72.4%)	340 (68.3%)	

TCGA-BLCA	Low (n=226)	High (n=272)	Total (n=498)	P value
Positive	25 (11.1%)	32 (11.8%)	57 (11.4%)	
Perineural_invasion_present**				0.0024
No	93 (41.2%)	92 (33.8%)	185 (37.1%)	
Yes	56 (24.8%)	109 (40.1%)	165 (33.1%)	
Smoking Status				0.4229
Light/Non-smoker	68 (30.1%)	72 (26.5%)	140 (28.1%)	
Smoker	157 (69.5%)	198 (72.8%)	355 (71.3%)	
TMB				0.8414
High	65 (28.8%)	75 (27.6%)	140 (28.1%)	
Low	161 (71.2%)	197 (72.4%)	358 (71.9%)	
ATGcluster***				<0.00001
ATGclusterA	77 (34.1%)	98 (36.0%)	175 (35.1%)	

TCGA-BLCA	Low (n=226)	High (n=272)	Total (n=498)	P value
ATGclusterB	54 (23.9%)	2 (0.7%)	56 (11.2%)	
ATGclusterC	40 (17.7%)	103 (37.9%)	143 (28.7%)	
ATGclusterD	47 (20.8%)	44 (16.2%)	91 (18.3%)	
ATGclusterE	8 (3.5%)	25 (9.2%)	33 (6.6%)	
New tumor event				0.3971
No	152 (67.3%)	164 (60.3%)	316 (63.5%)	
Yes	54 (23.9%)	71 (26.1%)	125 (25.1%)	
Mutation in <i>TP53</i>***				<0.00001
Mutation	119 (52.7%)	215 (79.0%)	334 (67.1%)	
WT	107 (47.3%)	57 (21.0%)	164 (32.9%)	
Mutation in <i>CDKN2A</i>**				0.0047
Mutation	32 (14.2%)	67 (24.6%)	99 (19.9%)	

TCGA-BLCA	Low (n=226)	High (n=272)	Total (n=498)	P value
WT	194 (85.8%)	205 (75.4%)	399 (80.1%)	

Table S3. Summary of detailed clinical information of the IMvigor210 (mUC) cohort.

IMvigor210 cohort	Low (n=204)	High (n=144)	Total (n=348)	P value
Sex				1
Female	45 (22.1%)	31 (21.5%)	76 (21.8%)	
Male	159 (77.9%)	113 (78.5%)	272 (78.2%)	
Vital status				0.000032
Alive	86 (42.2%)	30 (20.8%)	116 (33.3%)	
Dead	118 (57.8%)	114 (79.2%)	232 (66.7%)	

IMvigor210 cohort	Low (n=204)	High (n=144)	Total (n=348)	P value
Overall response				0.000746
CR	19 (9.3%)	6 (4.2%)	25 (7.2%)	
PR	33 (16.2%)	10 (6.9%)	43 (12.4%)	
SD	42 (20.6%)	21 (14.6%)	63 (18.1%)	
PD	82 (40.2%)	85 (59.0%)	167 (48.0%)	
Binary response				0.000889
CR/PR	52 (25.5%)	16 (11.1%)	68 (19.5%)	
SD/PD	124 (60.8%)	106 (73.6%)	230 (66.1%)	
Enrollment IC				< 0.00001
IC0	36 (17.6%)	63 (43.8%)	99 (28.4%)	
IC1	83 (40.7%)	49 (34.0%)	132 (37.9%)	

IMvigor210 cohort	Low (n=204)	High (n=144)	Total (n=348)	P value
IC2	85 (41.7%)	32 (22.2%)	117 (33.6%)	
TC Level				0.600617
TC0	164 (80.4%)	111 (77.1%)	275 (79.0%)	
TC1	13 (6.4%)	9 (6.2%)	22 (6.3%)	
TC2	26 (12.7%)	24 (16.7%)	50 (14.4%)	
Immune phenotype				< 0.00001
desert	25 (12.3%)	51 (35.4%)	76 (21.8%)	
excluded	91 (44.6%)	43 (29.9%)	134 (38.5%)	
inflamed	54 (26.5%)	20 (13.9%)	74 (21.3%)	
Lund1				0.020422
MS1a	12 (5.9%)	11 (7.6%)	23 (6.6%)	

IMvigor210 cohort	Low (n=204)	High (n=144)	Total (n=348)	P value
MS1b	33 (16.2%)	46 (31.9%)	79 (22.7%)	
MS2a1	31 (15.2%)	14 (9.7%)	45 (12.9%)	
MS2a2	21 (10.3%)	4 (2.8%)	25 (7.2%)	
MS2b1	63 (30.9%)	29 (20.1%)	92 (26.4%)	
MS2b2.1	11 (5.4%)	7 (4.9%)	18 (5.2%)	
MS2b2.2	33 (16.2%)	33 (22.9%)	66 (19.0%)	
Lund2				.000232
Basal/SCClike	33 (16.2%)	33 (22.9%)	66 (19.0%)	
Genomically unstable	52 (25.5%)	18 (12.5%)	70 (20.1%)	
Infiltrated	63 (30.9%)	29 (20.1%)	92 (26.4%)	
UroA	45 (22.1%)	57 (39.6%)	102 (29.3%)	

IMvigor210 cohort	Low (n=204)	High (n=144)	Total (n=348)	P value
UroB	11 (5.4%)	7 (4.9%)	18 (5.2%)	
TCGA				.027063
I	61 (29.9%)	57 (39.6%)	118 (33.9%)	
II	67 (32.8%)	28 (19.4%)	95 (27.3%)	
III	36 (17.6%)	33 (22.9%)	69 (19.8%)	
IV	40 (19.6%)	26 (18.1%)	66 (19.0%)	

Table S4. The relative amount of indicated TIME immune cells infiltration in TCGA-HNSCC cohort.

<https://drive.google.com/file/d/1VbTYRcu5RQWneRCH84lDJoMzyFt3trZ6/view?usp=sharing>

Table S5. Summary of ssGSEA for specific gene sets to represent biological processes related with stromal-activation, immune-activation and DNA damage repair (DDR) in TCGA-HNSCC cohort.

https://drive.google.com/file/d/15Wjv--Y3x_Ds274O1IJhoCT6f1sjcU6k/view?usp=sharing

<https://doi.org/10.17305/bb.2023.9094>

Table S6. The relative amount of indicated TIME immune cells infiltration in meta-HNSCC cohort.

<https://drive.google.com/file/d/1stq52pXHnyIM0BH94BTg4IJmgBMVdl01/view?usp=sharing>

Table S7. Summary of ssGSEA for specific gene sets to represent biological processes related with stromal-activation, immune-activation and DNA damage repair (DDR) in meta-HNSCC cohort.

<https://drive.google.com/file/d/1YiPgPX17feJBjJFxmzrzi-OaQVf0Yd5/view?usp=sharing>

Table S8. Summary of differential expression genes (DEGs) among five distinct autophagy related patterns through edgeR algorithm in TCGA-HNSCC cohort.

<https://docs.google.com/spreadsheets/d/12sOS6gO2EB2s8v7XX4sEd-r1xFFhZEPe/edit?usp=sharing&oid=111634499466144347170&rtpof=true&sd=true>

Table S9. The summary of univariate cox regression analyses of autophagy phenotype related genes in TCGA-HNSCC cohort.

https://docs.google.com/spreadsheets/d/1BKlOMslgnT22r0Di_Dd_VwvFGwM2NB-8/edit?usp=sharing&oid=111634499466144347170&rtpof=true&sd=true

<https://doi.org/10.17305/bb.2023.9094>

Table S10. The correlation between ATPscore and gene signatures linked to stromal-activation, immune-activation and DNA damage repair (DDR) in TCGA-HNSCC cohort.

https://drive.google.com/file/d/1r4_3wAkLaLavj_Hf2UuO7slGUWbd8n56/view?usp=sharing

Table S11. The relative amount of indicated TIME immune cells infiltration in microarray-HNSCC cohort.

https://drive.google.com/file/d/1bvYtB1vTI59_n_kxx4T-kcYdD-xhIriZ/view?usp=sharing

Table S12. Summary of ssGSEA for specific gene sets to represent biological processes related with stromal-activation, immune-activation and DNA damage repair (DDR) in microarray-HNSCC cohort.

<https://drive.google.com/file/d/1wYwh4KxtVyskpaf3v3yLa-fEvsKrDTB-/view?usp=sharing>

Table S13. The correlation between ATPscore and amount of TIME immune cells in microarray-HNSCC cohort.

<https://drive.google.com/file/d/1NTKKQHqvVOTDb5doguRihf5iMYDNfbZx/view?usp=sharing>

Table S14. The output of univariate and multivariate analyses for ATPscore and clinical parameters.

https://docs.google.com/spreadsheets/d/1Kbpg8AuPyGoMv_R30eeS0Ir1Frt4ePIF/edit?usp=sharing&oid=111634499466144347170&rtpof=true&sd=true

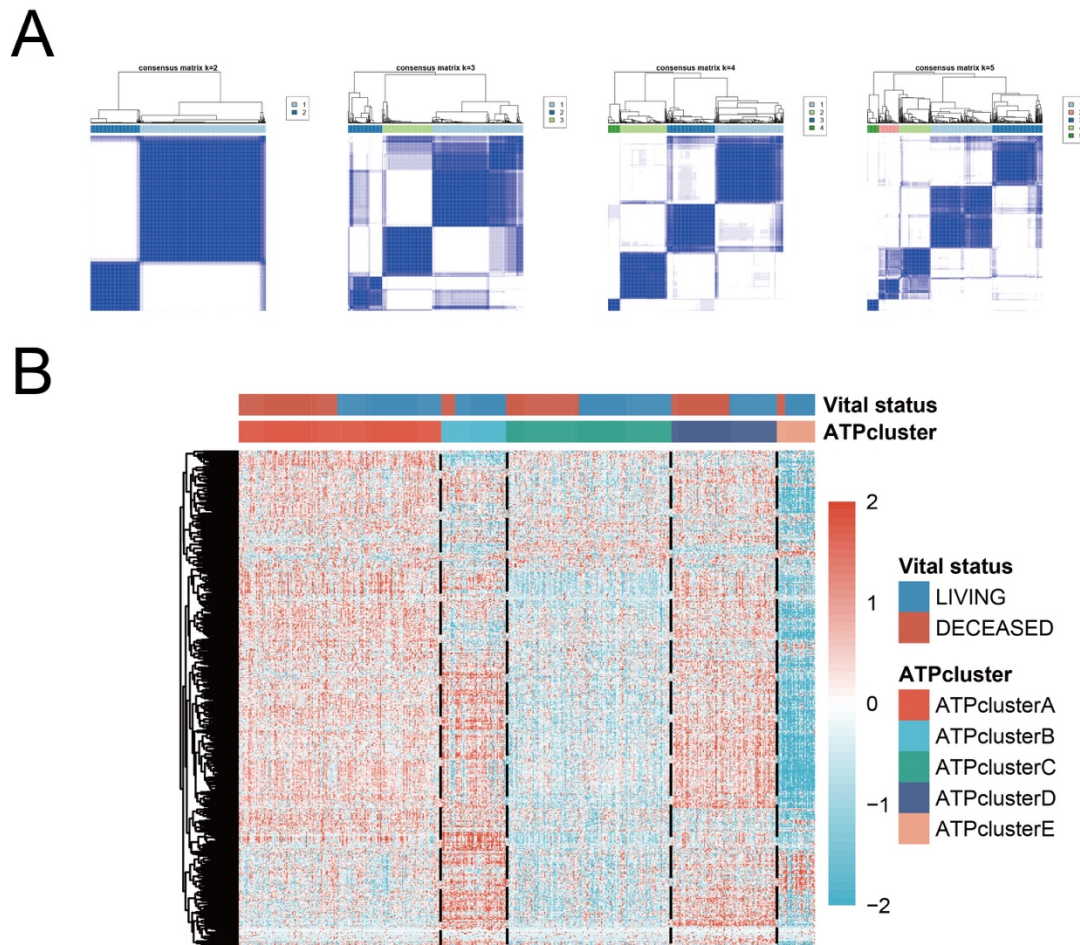


Figure S1. Consensus clustering of autophagy related genes in TCGA-HNSCC cohort.

(A) Consensus matrices of patients in TCGA-HNSCC cohort for $k = 2-5$ using 1000 iterations of unsupervised consensus clustering method (K-means) to ensure the clustering stability. (B) Hierarchical clustering of ATGs based on Euclidean distance and Ward linkage in TCGA-HNSCC cohort. The ATPclusters and vital status are shown as patient annotations. Rows represent ATGs, and columns represent HNSCC samples. Red represents genes which were relatively upregulated, and blue represents genes relatively downregulated.

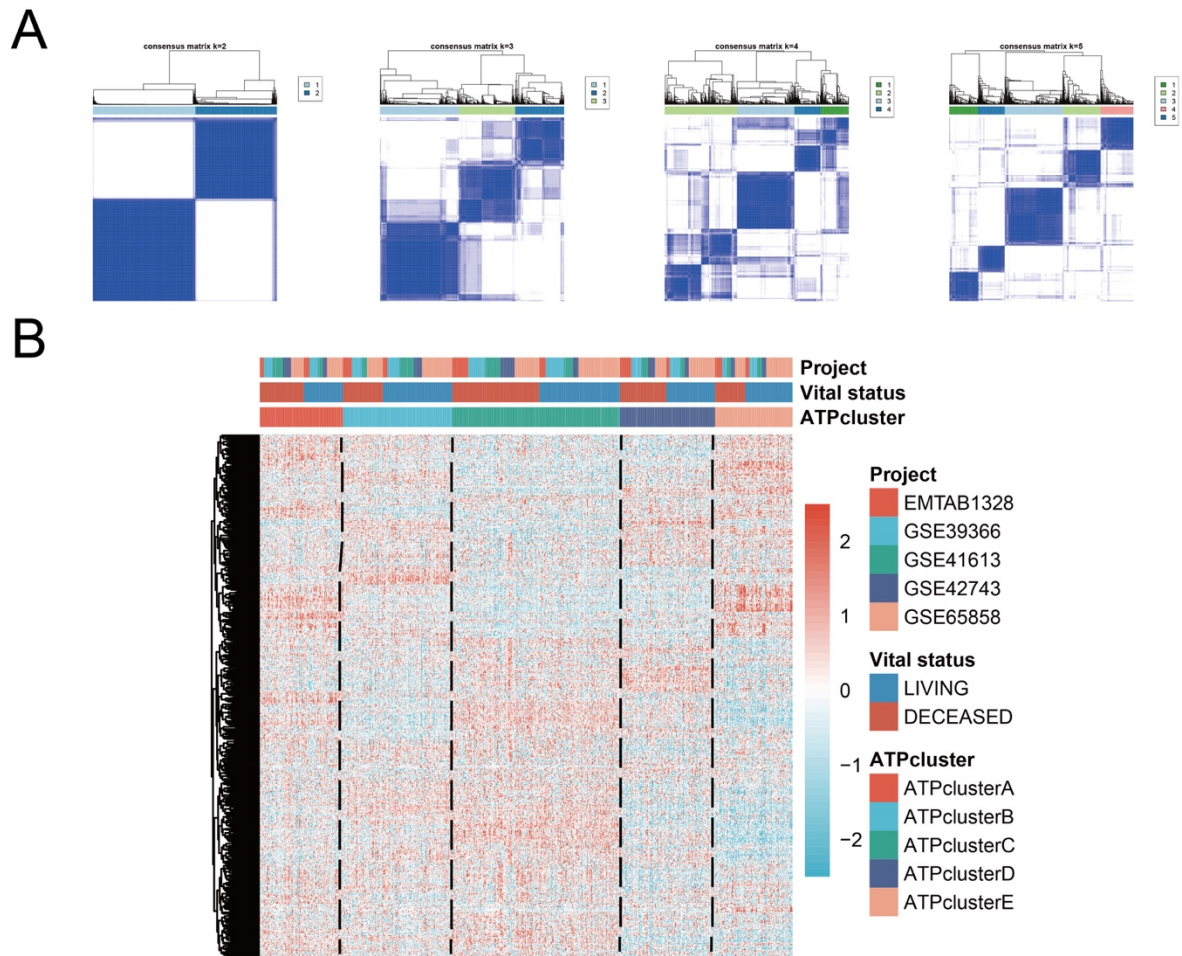


Figure S2. Consensus clustering of autophagy related genes in meta-HNSCC cohort. (A) Consensus matrices of patients in meta-HNSCC cohort for $k = 2-5$ using 1000 iterations of unsupervised consensus clustering method (K-means) to ensure the clustering stability. (B) Hierarchical clustering of autophagy related genes based on Euclidean distance and Ward linkage in meta-HNSCC cohort. ATPclusters, vital status, and projects are shown as patient annotations. Rows represent ATGs, and columns represent HNSCC samples. Red represents genes which were relatively upregulated, and blue represents genes relatively downregulated.

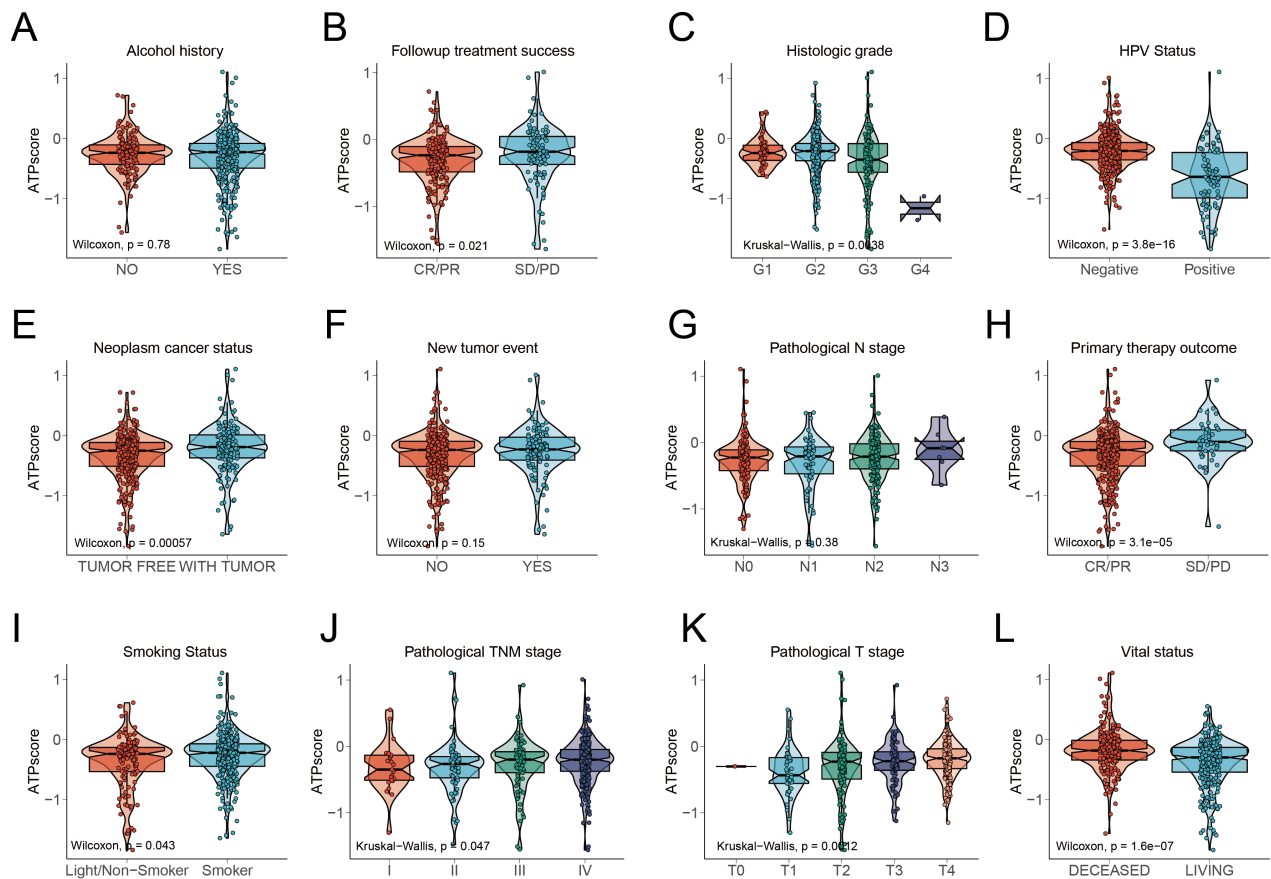


Figure S3. Differences of ATPscore among different clinical features in TCGA-HNSCC cohort. The upper and lower ends of the boxes represented interquartile range of values. The lines in the boxes represented median value. Wilcoxon tests and Kruskal-Wallis tests were used to compare the statistical difference between alcohol history (A), follow-up treatment success (B), histological grade (C), HPV status (D), neoplasm cancer status (E), new tumor event (F), pathological N stage (G), primary therapy outcome (H), smoking status (I), pathological TNM stage (J), pathological T stage (K), and vital status (L).

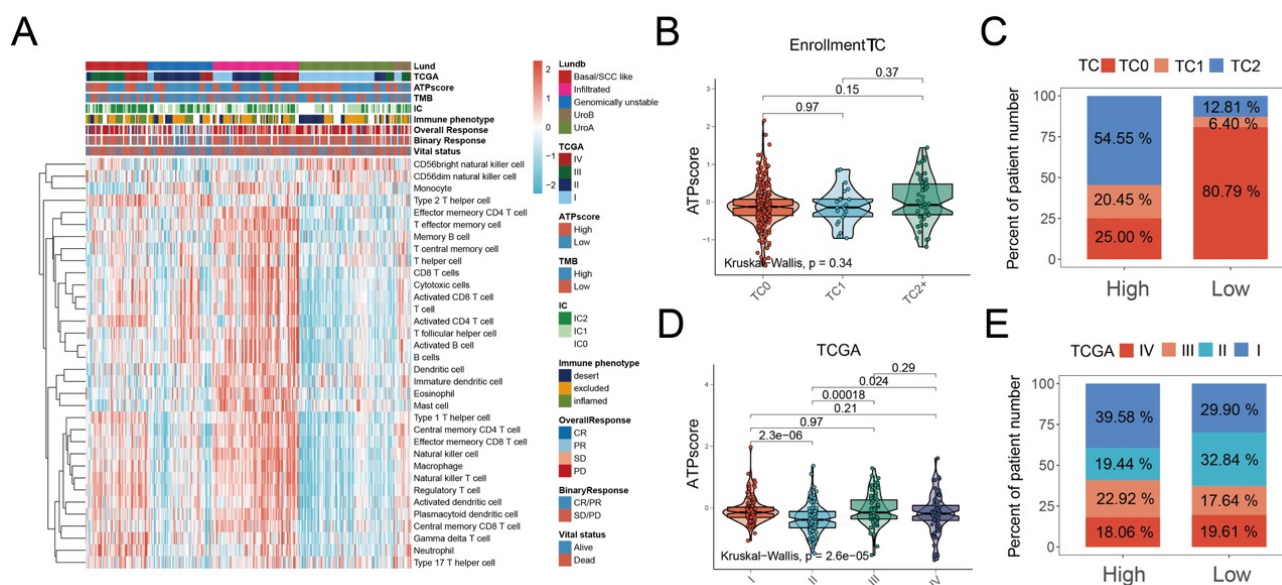


Figure S4. The biological characteristics and predictive value of ATPscore in the IMvigor210 (mUC) cohort. (A) Hierarchical clustering of TIME landscape in the IMvigor210 (mUC) cohort. Rows represent relative amount of each immune cell, and columns represent samples. Red represents the amount of immune cells which were relatively upregulated and blue represents immune cells relative downregulated. (B) Differences in ATPscore among different PD-L1 expression on tumor cells (TC) in the IMvigor210 (mUC) cohort. The Kruskal-Wallis test was used to compare the statistical difference between different TC0-TC2 groups (Kruskal-Wallis test, $P = 5.5e-9$, Kruskal-Wallis test, $P = 0.34$). (C) The proportion of TC subtypes between high and low ATPscore groups in IMvigor210 (mUC) cohort. The statistical difference was measured with the Fisher's exact test. (Fisher's exact test, $P = 0.728113$). (D) Differences in ATPscore among different molecular subtypes in TCGA molecular classification system in IMvigor210 (mUC) cohort. The Kruskal-Wallis test was used to compare the statistical difference among different molecular subtypes (Kruskal-Wallis test, $P = 2.6e-5$). (E) The proportion of TCGA molecular subtypes between the high and low ATPscore groups in IMvigor210 (mUC) cohort. The statistical difference was measured with the Fisher's exact test. (Fisher's exact test, $P = 0.116173$).